



1. Introduction

A robust intensity measure (IM) can be defined as one that has the ability to provide stable (and unbiased) structural response estimates when different sets of ground motions are used in structural performance assessments. This enables different engineers to arrive to similar conclusions regarding the seismic performance of a given structural model. Robustness is achieved by a combination of an IM with adequate efficiency [1], sufficiency [2] with respect to various ground motion characteristics that have an influence on the IM, and a small or negligible sensitivity of the IM to changes in the scale factors used to reach the target intensities.

For sites located near active faults and with certain geometry characteristics relative to the fault and its rupture process, ground motions can exhibit strong directivity effects characterized by severe long-duration acceleration pulses that tend to produce large lateral deformations demands on structures that may trigger collapse (e.g., [3-11]). In the near-fault region, these long-duration acceleration pulses, which also produce large velocity pulses, are primarily a consequence of forward-directivity effects resulting from seismic energy arriving at the site practically at the same instant of time as a result of the rupture propagating towards a site at a velocity similar to the shear wave velocity [12]. The type of ground motions exhibiting this ‘strong’ pulse are commonly referred to as near-fault pulse-like (NFPL) ground motions.

Some of the first recorded earthquakes that presented this distinctive ‘strong’ pulse feature were the 1957 M_s 4.7 Port Hueneme earthquake [13], the 1966 M_w 6.2 Parkfield earthquake [14], and the 1971 M_w 6.6 San Fernando earthquake [15]. Even when the magnitudes of these early earthquakes are relatively low, NFPL generated long-duration acceleration pulses that caused considerable structural damage. Therefore, when assessing the seismic risk of structures built on sites located near faults, it is important to adequately characterize the hazard and risk associated to these ground motions.

The most commonly used IM to describe the intensity of a ground motion in probabilistic seismic hazard analysis, for defining seismic actions in seismic codes, and more recently to evaluate the seismic performance of structures is the 5%-damped pseudo-acceleration spectral ordinate at the fundamental period of vibration of the structure, S_a . Several researchers have proposed approaches to adjust ground motion prediction models (GMPM) and probabilistic seismic hazard analysis in near-source sites (e.g., [12,16-18]) in order to account for differences in elastic spectral ordinates from NFPL ground motions and what is often referred to as ‘ordinary’ ground motions (e.g., [7]). Many of these proposals assume that a continuum of acceleration time series that have a wide range of dominant pulse periods, durations, and amplitudes can be subdivided into a somewhat arbitrary binary classification of pulse-like and non-pulse-like or so-called ‘ordinary’ ground motions. These procedures have been proposed for ground motion selection at sites where pulse-like ground motions are likely to occur. They are also used in defining the proportion of expected pulse-like ground motions in a ground motion set, the probability distribution of the pulse period, T_p , and for determining target spectral shapes when selecting records to conduct the seismic performance assessment at a given hazard level. However, many studies have shown that nonlinear structures respond differently to pulse-like ground motions than elastic structures (e.g., [3-10]) and therefore estimating elastic spectral ordinates may lead to biased estimates of inelastic response of structures. Several other studies have found that S_a is not an adequate parameter to characterize the damage potential of pulse-like ground motions as this IM has been found not sufficient with respect to T_p (e.g., [10, 19, 20]). Furthermore, using S_a as the IM when NFPL ground motions are expected to occur at the site may lead to a large dispersion of the engineering demand parameter (EDP). This causes a reduction in the confidence in the estimation obtained with a small number of ground motions, or requiring a very large number of ground motions to obtain reliable estimates of the probability of collapse.

Hence, it is of paramount importance to identify or develop sufficient and efficient IMs that can provide more accurate nonlinear response estimates for sites where NFPL are likely to occur (e.g., reducing the probability of producing biased response estimates and avoiding the use of very large ground motion data sets) while, at the same time, simplifying the record selection process. A desired simplification in record selection would be not having to select records from binarily classified ground motions, not requiring to match specific



target proportions of either ‘pulse-like’ or ‘ordinary’ ground motions, or not having to select ground motions within very narrow ranges of magnitude, duration, or other ground motion characteristics.

In order to overcome some of the limitations of using S_a as an IM, Baker and Cornell [21] proposed the use of a vector IM consisting of S_a and ε , where the latter is defined as the number of standard deviations that the logarithm of the spectral ordinate from a ground motion differs from the mean estimation of a GMPM. However, in a subsequent study they concluded that ε was ineffective at accounting for the effect of velocity pulses in NFPL ground motions as results were sensitive to the ratio of the pulse period to T_l . The T_p/T ratio will be referred to hereafter as pulse ratio (PR). Haselton et al. [22] developed an approximate method to account for the effects of spectral shape by using the scalar IM S_a , but adjusted by the difference between the target ε at the site and the values of ε of the records used in the evaluation. This ε -adjusted S_a hereafter is referred to as $S_{a+\varepsilon}$. However, similarly to the previous study they found that $S_{a+\varepsilon}$ did not yield good results when used with NFPL ground motions and warned that their method ‘should not be applied to near-fault motions with large forward-directivity velocity pulses’. Despite the warning, their approximate method was adopted in the FEMA P695 methodology [23]. Not being able to use their approximate method with satisfactory results for NFPL ground motions is a major shortcoming because these type of ground motions are those that are most likely to produce large intensities leading to large probabilities of structural collapse for structures located close to active faults. Therefore, IMs that can be used with NFPL ground motions are preferred.

Recognizing the limitations of the use of either S_a or the vector IM $\{S_a, \varepsilon\}$ in the probabilistic seismic demand analysis of structures subjected to pulse-like ground motions, many researchers have proposed alternative scalar or vector IMs (e.g. [2, 19, 20, 24]). Similarly, Eads et al. [25, 26] proposed and evaluated the use of $S_{a_{avg}}$, defined as the geometric mean of pseudo-spectral accelerations in a range of periods between one-fifth and three times T_l . They found that $S_{a_{avg}}$ provided fairly similar collapse risk estimates of a four-story steel moment frame when subjected to seven different ground motion sets, some of which included a large proportion of pulse-like ground motions and one of them containing exclusively NFPL ground motions according to the binary classification proposed in [18]. Moreover, $S_{a_{avg}}$ was found to be significantly more efficient and more sufficient with respect to several ground motion parameters than the IMs S_a and $S_{a+\varepsilon}$. However, they did not evaluate the sufficiency of $S_{a_{avg}}$ with respect to PR . Tarbali et al. [27] concluded that a ground motion selection procedure based on an appropriate set of intensity measures leads to an accurate representation of the seismic hazard of sites in the near-fault region and alleviates the need to specify the proportion of pulse-like motions and their pulse periods.

More recently, the authors proposed a new scalar IM, referred to as $FIV3$, specifically aimed at collapse risk estimation [28, 29]. This IM is based on a period-dependent version of the incremental velocity proposed by Bertero and his co-workers during the 70s and 80s [3, 4] which considers the three pulse segments with the largest area under the acceleration pulse that are acting on the same direction and which are extracted from a low-pass filtered acceleration time series. Results from structural collapse assessments using seven moment-resistant frame structures with periods of vibration ranging from 0.42s to 2.36s when using a base set of 272 ground motions suggest that this IM is highly efficient. Moreover, comparisons of the sufficiency of $FIV3$ and that of several other traditional and advanced IMs with respect to five different ground motion parameters indicates that this IM is well suited for seismic collapse risk estimation. Nonetheless, the sufficiency of $FIV3$ with respect to PR and its robustness when using various ground motion sets was not investigated.

The main objectives of this study are: (1) to evaluate the efficiency and sufficiency of $FIV3$ with respect to PR using NFPL ground motions; and (2) to assess the robustness of $FIV3$ by evaluating the sensitivity of collapse fragility curves and mean annual frequencies of collapse computed using six different ground motion sets that include different proportions of non- and pulse-like ground motions. The performance of $FIV3$ is compared with the two most commonly used scalar IMs, namely S_a and $S_{a+\varepsilon}$, and with $S_{a_{avg}}$.



2. Structures and sets of ground motions

In this study, collapse results from two 4-story MDOF structures modeled in the OpenSees platform [30] are used in the evaluation of the efficiency, sufficiency, and robustness of the four IMs using sets of ground motions containing pulse- and non-pulse-like ground motions.

The first structure corresponds to a reinforced concrete (RC) moment resisting frame (MRF) structure designed and modeled by Haselton and Deierlein [31] and identified by the code ID 1008 from now on. It consists of a two-dimensional model with a fundamental period of vibration of 0.94s, which incorporates finite joint shear panels and concentrated plasticity elements at the ends of beams and columns whose hysteretic behavior is characterized by a modified Ibarra-Medina-Krawinkler model calibrated for ductile RC structures. For a detailed description of the structural model, the reader is referred to [31].

The second structure is a two-dimensional steel moment-resisting frame structure with reduced beam sections at the ends of the beams designed by Lignos and Krawinkler [32] and modeled in OpenSees by Eads and Miranda [26]. This structure has a fundamental period of vibration of 1.33s. Its hysteretic behavior consists of zero-length nonlinear rotational springs located at the center of the RBS locations in the case of beams and at the edges of the column panel zones for the columns. A detailed description of this structural model can be found in [26, 32]. This model will be identified by the code ID 5000 hereafter.

Nonlinear response history analyses were conducted on both structures when subjected to six different ground motion sets. The ground motions in all sets are ground motions recorded during various earthquakes selected from the NGA-West2 ground motion database [33].

The first ground motion set consists of the 137 record pairs compiled and used in [25, 26]. The moment magnitudes, M_w , of these records range between 6.93 and 7.62 and Joyner-Boore distances, R_{jb} , defined as the distance from the recording station to the surface projection of the fault rupture, vary between 0 and 27km. All the ground motions in this set were recorded in stations located in NEHRP site classes C or D. According to the method proposed by Shahi and Baker [34], thirty four percent of the records in this ensemble present forward directivity characteristics. This ground motion set is hereafter referred to as the MRCD* set. For this and the rest of the sets, the method proposed in [34] is used to classify a ground motion as a pulse-like.

The second ground motion set consists of 234 records that do not present non-pulse-like features in any orientation. Their M_w ranges between 5.9 and 7.9, their R_{jb} between 0 and 246, and are obtained from stations located on NEHRP site classes C and D. This record set will be referred to as the 'Non-pulse-like set' hereafter.

The third set is called 'Extended FEMA set' and corresponds to the ground motion records compiled in Haselton and Deierlein [31] which consists of 39 pairs of recordings from events with M_w between 6.50 and 7.62 and R_{jb} between 0.9 and 74.2 km. The reader is referred to Appendix 3B in [31] for additional details about this record set

From all the records in the NGA-West2 database that were classified as pulse-like ground motions, 234 were available from the website and were used to assemble the last three sets. The fourth and fifth sets, termed 'FN set' and 'FP set' correspond to the fault normal (FN) and fault parallel (FP) components, respectively, whereas the sixth set, referred to as 'Max Pulse set' corresponds to the same recordings but rotated to the orientation at which the 'strongest' or 'maximum' velocity pulse was found. The rotation angle required for each recording in the three set cases is provided in [35]. All these records were obtained from stations located on NEHRP site classes A, B, C, and D, their magnitudes range between 5 and 7.9, and Joyner-Boore distances vary between 0 and 92.6 km.



Results from all subsequent analyses were only considered if the scale factor required to trigger collapse was equal or lower than 5. This decision was based on previous studies supporting the adequacy of this upper limit in scale factor for this type of structures [28, 29] when *FIV3* is used as the IM.

3. *FIV3* definition

This study used the *FIV3* definition proposed in [29] and is repeated here for the sake of clarity:

$$FIV3 = \max\{V_{s,max1} + V_{s,max2} + V_{s,max3}, |V_{s,min1} + V_{s,min2} + V_{s,min3}|\} \quad (1)$$

$$V_s(t) = \left\{ \int_t^{t+0.7 \cdot T_n} \ddot{u}_{gf}(\tau) d\tau, \forall t < t_{end} - \alpha \cdot T_n \right\} \quad (2)$$

where $V_{s,max1}$, $V_{s,max2}$, and $V_{s,max3}$, are the first, second, and third local maximum incremental velocities computed by accumulating ground accelerations in a time segment with duration $0.7 \cdot T_n$ starting at time t , respectively, and similarly $V_{s,min1}$, $V_{s,min2}$, and $V_{s,min3}$, are the first, second, and third local minimum incremental velocities computed accumulating ground accelerations over durations of $0.7 \cdot T_n$, respectively. T_n corresponds to the fundamental period of vibration of the structure, and \ddot{u}_{gf} to the ground acceleration time series filtered using a 2nd order Butterworth low-pass filter with a cut-off frequency of 1.0 Hz.

4. Efficiency evaluation

Efficiency is defined as the ability of an IM to estimate structural responses with a small variability [1]. In this study, these structural responses correspond to ground motion intensities producing collapse. The efficiency of *FIV3* was compared against other three scalar IMs: S_a , $S_a + \varepsilon$, and $S_{a,avg}$ as proposed in [25, 26]. For the computation of the ε values for each ground motion the 2008 Boore and Atkinson GMPM [36] was used. These values were then used to adjust the S_a -based collapse capacities following the procedure recommended in [22, 23].

Figure 1 presents the logarithmic standard deviation (σ_{nIM}) of the four IMs using the six ground motion sets and for the two four-story structures. The left panel presents the comparison for the RC structure while right panel presents the corresponding results for the steel structure. In both cases, the largest variabilities were computed when S_a is used as IM which means that it is the least efficient IM. Using advanced IMs such as $S_{a,avg}$ and *FIV3* lead to much smaller variabilities. In these cases, with respect to σ_{nS_a} , average reductions in σ_{nIM} of 49% are achieved by using *FIV3*.

The benefit of this reduction in dispersion means that the number of nonlinear response history analyses (NRHA) required to provide structural collapse estimates with a given confidence level is reduced. For example, for the same standard error, if *FIV3* is used as the IM, one only needs to conduct approximately one-fourth and one-third of the NRHA required with S_a and $S_a + \varepsilon$, respectively. In other words, the computational effort associated with the same confidence in the median collapse capacity is reduced by a factor of almost 4 by using *FIV3* in lieu of S_a and by a factor of 3 with respect to $S_a + \varepsilon$.

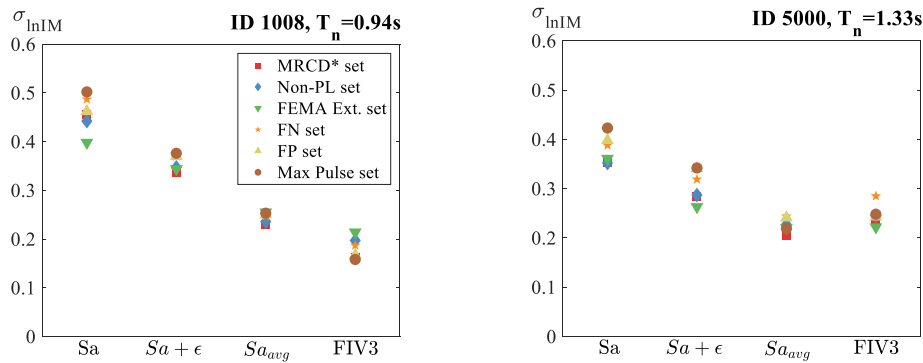


Fig. 1 – Efficiency comparison of scalar IMs as measured by the logarithmic standard deviation of collapse intensities computed when using the six ground motion sets: (a) RC structure; and (b) Steel structure.

4. Sufficiency evaluation with respect to pulse-period ratio

The adequate sufficiency of *FIV3* with respect to M_w , source-to-site-distance, spectral shape, duration, and scale factor was validated in previous studies using several moment resisting frame structures [28, 29]. This study assesses its sufficiency with respect to the pulse period ratio (PR), T_p/T_l .

The simplified relative sufficiency (SRS) approach proposed in [28, 29] was used in this study and it consists of conducting a standard linear regression on the normalized collapse intensities (with respect to its median) of a structural model against the ground motion characteristic of interest and then using the absolute value of the slope to compare the sufficiency of each IM. Following this approach, an IM is said to be more sufficient IM if it has a smaller absolute value of the slope (S) as this value provides a direct measure of the level of bias that can be introduced in the structural collapse capacity with a unitary change in the ground motion characteristic.

Figure 2 presents the SRS evaluation of the four IMs with respect to PR ratio using the four-story steel structure when subjected to 180 NFPL records rotated in the direction at which the ‘strongest’ velocity pulse was observed and whose PR ranged between 0.3 and 5. The largest slope (S_{PR}) corresponds to that computed when S_a is used as IM followed by the one computed using $S_a + \epsilon$. This means that these are the two least sufficient IMs with respect to PR of the four IMs evaluated in this study. These relatively large slopes indicate that structural collapse intensities are significantly influenced by the T_p/T_l values of the ground motions selected to conduct the NRHA, with a strong tendency for collapse intensities to decrease with increasing T_p/T_l . On the other hand, $S_{a,avg}$ and *FIV3* are IMs that lead to significantly smaller normalized slopes and therefore provide more stable values of collapse intensities as they are less affected by the ratio of the pulse period to the fundamental period of vibration of the structure. The sensitivity of $S_{a,avg}$ to changes in T_p/T_l is approximately one third of that computed when S_a is used as the IM. In particular, it is noteworthy that the normalized slope of *FIV3* is smaller than that computed when using S_a as the IM by a factor of approximately 6.5, meaning that, for this structure and set of records, *FIV3* is approximately 6.5 times more sufficient with respect to the pulse period ratio than S_a .

Results of the SRS evaluation of the four IMs with respect to PR for the four-story steel structure when using 153 pulse-like records whose PR was smaller than five followed similar trends as those presented in Figure 3. In that structure, the sufficiency of *FIV3* is three times larger than that of $S_{a,avg}$. Again, that the largest absolute normalized slopes, and therefore the least sufficient IMs for NFPL ground motions corresponded to S_a and $S_a + \epsilon$. Conversely, $S_{a,avg}$ and *FIV3* have much smaller normalized slopes.

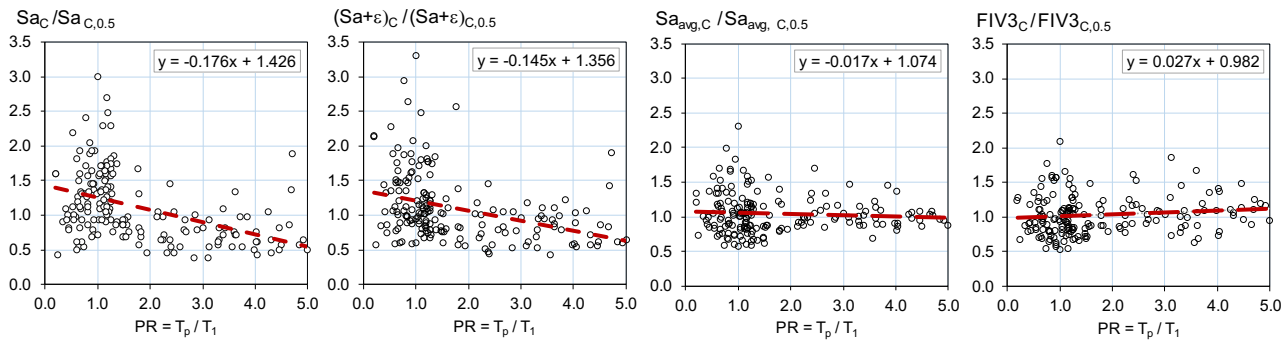


Fig. 2 – Sufficiency evaluation of the four scalar IMs with respect to the pulse period ratio when using a subset of the Max Pulse ground motion set in the 4-story steel structure.

Results from both structures suggest that S_{avg} and $FIV3$ are significantly less sensitive to changes in pulse period ratio (PR), T_p / T_1 , and therefore more sufficient with respect to the pulse period of the record relative to the fundamental period of vibration. By comparing the average S_{PR} from the two structural models, it is found that $FIV3$ is 8.3, 7.1, and 2.1 times more sufficient with respect to the pulse period ratio than S_a , $S_a + \varepsilon$, and S_{avg} , respectively. Therefore, by using $FIV3$ it is practically unnecessary to estimate the probability distribution of pulse periods as done in some previous investigations and therefore the use of $FIV3$ as an IM significantly simplifies the record selection procedure.

4. Robustness of $FIV3$ in estimating story drift ratios and collapse metrics

As mentioned previously, when using S_a as the IM, collapse intensities are influenced by or are sensitive to the pulse period ratio, T_p / T_1 . In particular, if S_a is used as the IM, collapse intensities show large reductions as T_p / T_1 increases. In order to evaluate the robustness of the estimation of story drift ratios $FIV3$ when using pulse-like ground motions having different pulse period ratios, the ‘Max Pulse’ set was further subdivided into two different suites of ground motions. The first subset, referred here as the *benign* set of pulse-like ground motion records, consists of records with $0.5 \leq T_p / T_1 \leq 1.5$. The second subset, referred here as the *damaging* set of pulse-like ground motion records, consists of records with $1.5 \leq T_p / T_1 \leq 5$. Figure 3a presents median peak interstory drift ratios as a function of IM computed by conducting incremental dynamic analyses on the four-story RC structure when using S_a as the IM, while Figure 3b shows similar information but now computed using $FIV3$. Note that if S_a is used as the IM, the median collapse intensity is strongly dependent on which set of ground motions is used in the analysis. Results indicate that collapse capacities in the *benign* and *damaging* sets differ only by 11% when using $FIV3$ as IM compared to a factor of 1.95 when using S_a as the IM.

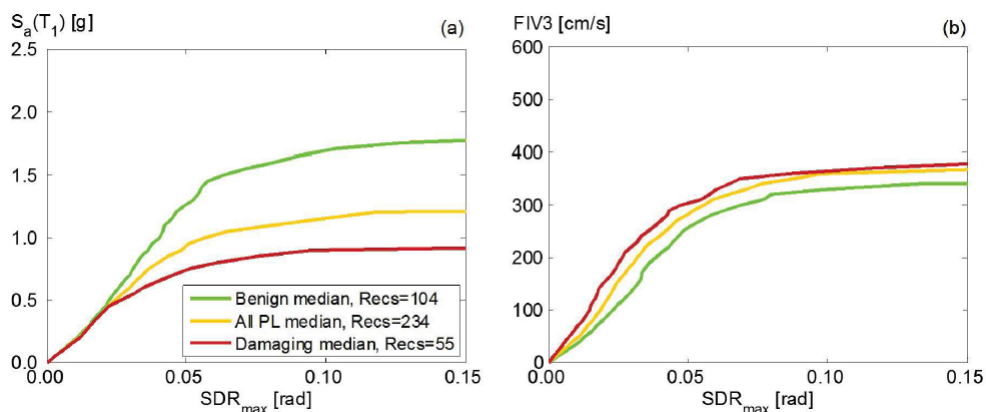


Fig. 3 – Median IDA curves computed using different subsets of the Max. Pulse set for the ID 5000 steel structure.



For the robustness evaluation of collapse metrics, the same hypothetical site used in [25, 26] was selected for the computation of the mean annual frequencies of collapse, λ_c , in this and the remaining sections of this paper. This site is assumed to be located at 10km from the rupture of a strike-slip fault, thus $R_{jb} = 10$ km. Its magnitude distribution is characterized by the bounded Gutenberg-Richter recurrence law with $6 < M_w < 8$ and the mean annual rupture rate is taken as $\lambda(M > 6) = 0.02$. The average shear wave velocity at the site is $V_{s30} = 285$ m/s. The hazard curves for $S_{a_{avg}}$ and $FIV3$ are computed using recently developed GMPMs presented in [37, 38]. For the computation of the target ε for each suite of records, collapse deaggregations using the collapse fragility curve (CFC) were conducted to identify the moment magnitude, M_w , with the largest contribution to λ_c . Then, the identified M_w was used to find the target ε . In both structures, the target ε 's correspond to 1.35 and 2.28.

Figure 4 presents results of the median collapse capacities obtained for each of the IMs and the six suites of ground motions normalized by the mean collapse capacity ($\overline{IM}_{C,0.5}$) of the six sets from the corresponding IM. Results corresponding to the $T_l = 0.94$ s RC structure (ID 1008) are presented in Figure 4a whereas Figure 4b presents the results for the $T_l = 1.33$ s steel structure (ID 5000). In general, it is seen that the median collapse capacities show a much smaller sensitivity to the ground motion set used when using $FIV3$ as the IM than when using either S_a or $S_a + \varepsilon$, that is, collapse intensities are much more stable using $FIV3$ than when using S_a or $S_a + \varepsilon$. While the median collapse capacity can differ by 44% among sets when using S_a as in IM, it only differs by 9% when using $FIV3$.

The comparison of the robustness of mean annual frequency of collapse (λ_c) computed when using the four IMs in the two models is presented in Figure 5. Mean annual frequencies of collapse computed using S_a as the IM, exhibit a very large variability, ranging from $1.2E-4$ to $4.49E-4$ in the case of 4-story RC structure (ID 1008), and from $1.61E-4$ to $3.46E-4$ in the case of of the 4-story steel structure (ID 5000). It can be seen the two more robust IMs, that is, those with the lower variability in λ_c estimates (i.e., less sensitivity in the mean annual frequency of collapse to the ground motion set used in the evaluation) are $S_{a_{avg}}$ and $FIV3$. The average COV in λ_c from S_a , $S_a + \varepsilon$, $S_{a_{avg}}$, and $FIV3$ corresponds to 0.34, 0.36, 0.26, and 0.20, respectively.

5. Influence of the proportion of pulse-like ground motion in median collapse capacities

Current proposals for structural performance assessment in the near-fault region require a somewhat arbitrary binary classification of ground motions into “pulse-like” and “non pulse-like” (also sometimes referred to as “ordinary”) and then recommend including specific proportions of pulse-like to “ordinary” records in the ground motion set based on the seismic hazard at the site (e.g., [39, 40]).

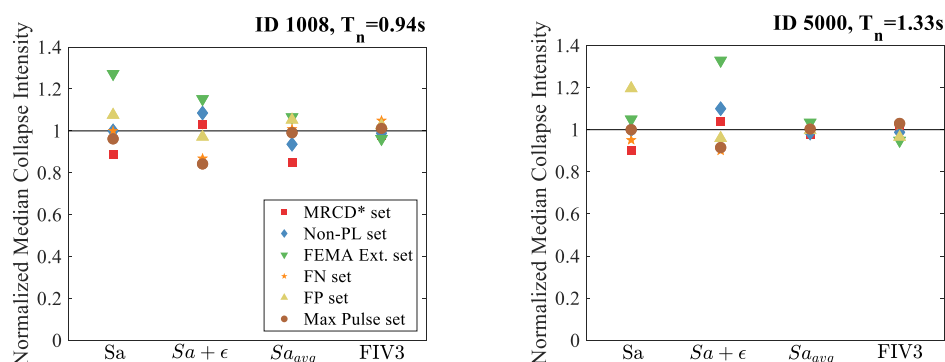


Fig. 4 – Evaluation of the robustness of four IMs in estimating median collapse capacities when using six different ground motion sets in each of the two structures.

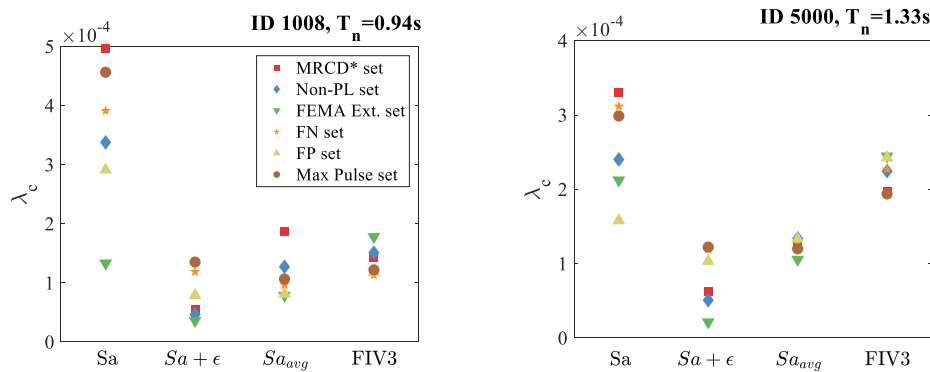


Fig. 5 – Evaluation of the robustness of four IMs in estimating mean annual frequencies of collapse when using six different ground motion sets in each of the two structures.

In order to evaluate the sensitivity of the results to the proportion of pulse-like ground motions used in the record set when using various IMs, a bootstrap analysis technique was used. The process consisted on estimating 3,000 collapse fragility curves by selecting 11 records from a pool of records consisting on a modified version of the 234 non-pulse-like ground motions and from the *benign* pulse-like record subset ($0.5 \leq PR \leq 1.5$) using five different target ratios of pulse-like to non-pulse-like ground motions ($R_{PL} = N_{PL}/N_{NPL}$), where N_{PL} and N_{NPL} correspond to the number of pulse-like and non pulse-like records, respectively. These target ratios are 0/11, 3/11, 6/11, 8/11, and 11/11. At an $R_{PL} = 0.5$, half of the 3,000 realizations considered 6 non-pulse-like records and 5 *benign* pulse-like records whereas the other half of the realizations considered 5 non-pulse-like records and 6 *benign* pulse-like records. The *benign* subset was chosen due to its relatively large difference in the median collapse capacity with respect to that computed from the non-pulse-like set.

Results of median collapse capacities normalized with respect to the median of the median collapse capacities of each IM computed using an $R_{PL} = 0.5$ are presented in Figure 6. As shown in this figure, when using S_a as IM, results are very sensitive to the fraction of pulse-like ground motions used in the set. For the RC structure, *FIV3* is the IM with the smallest sensitivity in normalized median collapse capacities caused by the fraction of *benign* pulse-like ground motion used. In the case of the steel structure (ID 5000), median collapse capacities computed using $S_{a_{avg}}$ are slightly less sensitive to the fraction of pulse-like records used in the record set, closely followed by *FIV3*. For all R_{PL} ratios the maximum deviation with respect to the median collapse capacity at a $R_{PL} = 0.5$ in both models equals 38.3%, 25.4%, 17.6%, and 10.1%, for S_a , $S_a + \epsilon$, $S_{a_{avg}}$, and *FIV3*, respectively. These results indicate that collapse risk estimations using *FIV3* are clearly less sensitive

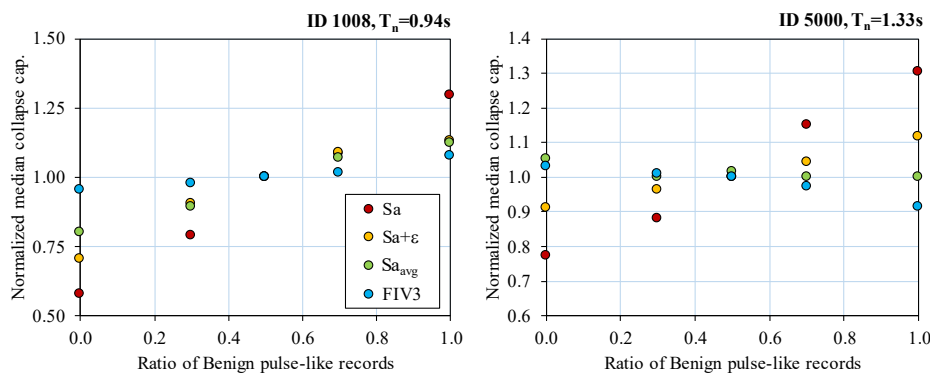


Fig. 6 – Normalized median collapse capacities obtained using different proportions of non-pulse-like and benign pulse-like ground motions. The normalization is with respect to the median of the corresponding IM computed using 50% of non-pulse-like and 50% of benign pulse-like records.



to the fraction of pulse-like ground motions included in the record set used in structural performance assessments. Hence, the record selection procedure required to assess the probability of collapse is greatly simplified as collapse risk estimates computed using *FIV3* are approximately the same whether only ‘ordinary’ ground motions are used, only pulse-like ground motion are used, or any fraction of pulse-like and ‘ordinary’ ground motion are used. Thus, procedures focusing on computing required target fractions of pulse-like ground motions, expected probability distribution of pulse periods conditioned on the IM, and strict ground motion selection criteria to match the target fractions of pulse-like ground motions and probability distributions of pulse periods are no longer necessary if *FIV3* is used as the IM, greatly simplifying the collapse assessment.

6. Conclusions

This study presented the robustness evaluation of a recently proposed IM referred to as *FIV3* when used in probabilistic seismic demand analysis of structures located near active faults by using results from two four-story structural models subjected to six different sets of ground motions. A wide range of pulse periods, durations, and amplitudes were used in the assessment as the sets used in this study range from 234 non-pulse-like records to 234 records rotated to the orientation at which the strongest velocity pulse was observed.

The performance of *FIV3* in terms of efficiency, sufficiency with respect to pulse period ratio, and robustness of collapse metrics was compared to that of two widely used scalar IMs, namely the 5%-damped spectral ordinate at the fundamental period, S_a , and the spectral ordinate at the fundamental period adjusted by the spectral shape proxy ε , $S_a + \varepsilon$, and to the recently proposed IM, $S_{a,avg}$. Finally, the sensitivity of median collapse intensities computed with *FIV3* when using suites of records with different fractions of pulse-like records was studied and compared against S_a , $S_a + \varepsilon$, and $S_{a,avg}$. From the results of these studies, the following conclusions are drawn:

1) The efficiency of *FIV3* is much larger than the one of S_a and $S_a + \varepsilon$ for all ground motion sets used in this investigation. The average reduction in variability of collapse intensities when using *FIV3* with respect to that computed using S_a and $S_a + \varepsilon$ in the two structural models and from the six ground motions sets considered herein are 48.8% and 42.3%, respectively. This means that using *FIV3* as IM requires a significantly smaller number of ground motions to achieve the same level of accuracy of the collapse estimate, or that for a given number of ground motions, the collapse estimate using *FIV3* will be more accurate than the one using the other two IMs.

2) *FIV3* was found to be much more sufficient with respect to the pulse period ratio than when using S_a and $S_a + \varepsilon$. This means that one can obtain approximately the same median collapse capacities whether by using ground motion set containing only pulse-like ground motions or by using ground motions set using only so called ‘ordinary’ ground motions or by using sets that have target proportions of these types of ground motions. Therefore, if *FIV3* is used as an IM, the record selection procedure is greatly simplified because it is no longer necessary to make use of relatively arbitrary binary classifications of ground motions, nor having to estimate target fractions of pulse-like ground motions and the target probability distribution of their pulse periods.

3) Collapse fragility curves and estimates of mean annual frequencies of collapse using a simple hypothetical site were found to be much more robust as they are significantly less sensitive to the particular suite of ground motions used in collapse assessment.

4) It was shown that when S_a is used as the IM, the estimation of median collapse intensities of these intermediate-period moment frame structures is strongly dependent on the fraction of pulse-like ground motions that are included in the ground motion set. On the other hand, median collapse intensities computed using *FIV3* as the IM were found to be relatively insensitive to the specific fraction of pulse-like ground motions included in the record set. These new results, together with those from previous studies [28, 29] indicate that *FIV3* is a very sufficient IM. The main two implications of this are: (i) more reliable results as they will be less affected by the characteristics of the specific records used in the analysis; and (ii) the use of *FIV3* provides more flexibility when selecting ground motions to be used in the nonlinear response history analyses as they do not need to satisfy very narrow ranges of magnitudes, distances, spectral shapes, or pulse periods.



7. Acknowledgements

The second author acknowledges the financial support from Consejo Nacional de Ciencia y Tecnología (CONACYT) in Mexico, and of the Blume-Gere Fellowship to pursue his doctoral studies at Stanford University under the supervision of the first author.

8. References

- [1] Shome N, Cornell CA, Bazzurro P, Carballo JE (1998). Earthquakes, records, and nonlinear responses. *Earthquake Spectra*, 14(3), 469-500.
- [2] Luco N, Cornell CA (2007). Structure-specific scalar intensity measures for near-source and ordinary earthquake ground motions. *Earthquake Spectra*, 23(2), 357-392.
- [3] Bertero VV, Mahin SA, Herrera RA (1978). Aseismic design implications of near-fault San Fernando earthquake records. *Earthquake Engineering and Structural Dynamics*, 6(1), 31-42.
- [4] Anderson JC, Bertero VV (1987). Uncertainties in establishing design earthquakes. *Earthquake Engineering and Structural Dynamics*, 113(8), 1709-1724.
- [5] Hall JF, Heaton TH, Halling MW, Wald DJ (1995). Near-source ground motion and its effects on flexible buildings. *Earthquake Spectra*, 11(4), 569-605.
- [6] Baez, JI, Miranda E (2000). Amplification factors to estimate inelastic displacement demands for the design of structures in the near field. *In Proceedings of the 12th World Conference on Earthquake Engineering*, Auckland, New Zealand.
- [7] Alavi B, Krawinkler H (2004). Behavior of moment-resisting frame structures subjected to near-fault ground motions. *Earthquake Engineering Structural Dynamics*, 33(6), 687-706.
- [8] Ruiz-García J, Miranda E (2004). Performance-based assessment of existing structures accounting for residual displacements. *The John A. Blume Earthquake Engineering Center Report No. 184*, Department of Civil and Environmental Engineering, Stanford University.
- [9] Akkar S, Yazgan U, Gülkan P (2005). Drift estimates in frame buildings subjected to near-fault ground motions. *Journal of Structural Engineering*, 131(7), 1014-1024.
- [10] Tothong P, Cornell CA (2008). Structural performance assessment under near-source pulse-like ground motions using advanced ground motion intensity measures. *Earthquake Engineering and Structural Dynamics*, 37(7), 1013-1037.
- [11] Iervolino I, Chioccarelli E, Baltzopoulos G (2012). Inelastic displacement ratio of near-source pulse-like ground motions. *Earthquake Engineering and Structural Dynamics*, 41(15), 2351-2357.
- [12] Somerville PG, Smith NF, Graves RW, Abrahamson NA (1997). Modification of empirical strong ground motion attenuation relations to include the amplitude and duration effects of rupture directivity. *Seismological Research Letters*, 68(1), 199-222.
- [13] Housner G, Hudson D (1958). The Port Hueneme earthquake of March 18, 1957. *Bulletin of Seismological Society of America*, 48(2), 163-168.
- [14] Housner G, Trifunac M. Analysis of accelerograms of Parkfield earthquake (1967). *Bulletin of Seismological Society of America*, 57(6), 1193-1220.
- [15] Mahin S, Bertero VV, Chopra AK, Collins R. Response of the Olive View hospital main building during the San Fernando earthquake (1976). *Report No. EERC 76-22*, University of California, Berkeley.
- [16] Tothong P, Cornell CA, Baker JW (2007). Explicit directivity-pulse inclusion in probabilistic seismic hazard analysis. *Earthquake Spectra*, 23(4), 867-891.
- [17] Iervolino I, Cornell CA (2008). Probability of occurrence of velocity pulses in near-source ground motions. *Bulletin of Seismological Society of America*, 98(5), 2262-2277.
- [18] Shahi SK, Baker JW (2011). An empirically calibrated framework for including the effects of near-fault directivity in probabilistic seismic hazard analysis. *Bulletin of Seismological Society of America*; 101(2), 742-755.
- [19] Tothong P, Luco N (2007). Probabilistic seismic demand analysis using advanced ground motion intensity measures. *Earthquake Engineering and Structural Dynamics*, 36(13), 1837-1860.



- [20] Baker JW, Cornell CA (2008). Vector-valued intensity measures for pulse-like near-fault ground motions. *Engineering Structures*, 30(4), 1048-1057.
- [21] Baker JW, Cornell CA (2005). A vector-valued ground motion intensity measure consisting of spectral acceleration and epsilon. *Earthquake Engineering and Structural Dynamics*, 34(10), 1193-1217.
- [22] Haselton CB, Baker JW, Liel AB, Deierlein GG (2009). Accounting for ground-motion spectral shape characteristics in structural collapse assessment through an adjustment for epsilon. *Journal of Structural Engineering*, 137(3), 332-344.
- [23] FEMA. Quantification of seismic performance factors (2009). *FEMAP-695 Report*, prepared by the Applied Technology Council for the Federal Emergency Management Agency, Washington, DC.
- [24] Bojorquez E, Iervolino I (2011). Spectral shape proxies and nonlinear structural response. *Soil Dynamics and Earthquake Engineering*, 31(7), 996-1008.
- [25] Eads L, Miranda E (2015). Average spectral acceleration as an intensity measure for collapse risk assessment. *Earthquake Engineering and Structural Dynamics*, 44(12), 2057-2073.
- [26] Eads L, Miranda E. Seismic collapse risk assessment of buildings: effects of intensity measure selection and computational approach (2013). *The John A. Blume Earthquake Engineering Center Report No. 184*. Department of Civil and Environmental Engineering, Stanford University.
- [27] Tarbali K, Bradley BA, Baker JW (2019). Ground motion selection in the near-fault region considering directivity-induced pulse effects. *Earthquake Spectra*, 35(2), 759-786.
- [28] Dávalos H, Miranda E (2019). Filtered incremental velocity: A novel approach in intensity measures for seismic collapse estimation. *Earthquake Engineering and Structural Dynamics*, 48(12), 1384-1405.
- [29] Dávalos H, Miranda E (2019). Evaluation of filtered incremental velocity, *FIV3*, as an intensity measure for estimating the probability of collapse of moment resisting frame buildings. Submitted for publication to *Journal of Structural Engineering*.
- [30] McKenna F, Fenves GL, Scott MH (2004). OpenSees: Open System for Earthquake Engineering Simulation. Pacific Earthquake Engineering Research Center, Berkeley, USA.
- [31] Haselton CB, Deierlein GG. Assessing Seismic Collapse Safety of Modern Reinforced Concrete Moment-Frame Buildings. *Technical report PEER 2007/08*, Pacific Earthquake Engineering Research Center, Berkeley USA.
- [32] Lignos DG, Krawinkler H (2012). Sidesway collapse of deteriorating structural systems under seismic excitations. *The John A. Blume Earthquake Engineering Center Report No. 177*. Department of Civil and Environmental Engineering, Stanford University.
- [33] NGA-West 2 project at: <<http://peer.berkeley.edu/ngawest2/>> (accessed: 03/10/18).
- [34] Shahi SK, Baker JW (2014). An efficient algorithm to identify strong-velocity pulses in multicomponent ground motions. *Bulletin of Seismological Society of America*, 104(5), 2456-2466.
- [35] <http://www.seismosoc.org/Publications/BSSA_html/bssa_104-5/2013191-esupp/pulse-like-records/2013191_esupp_Table_S2.html> (accessed: 01/23/20).
- [36] Boore DM, Atkinson GM. Ground-motion prediction equations for the average horizontal component of PGA, PGV, and 5%-damped PSA at spectral periods between 0.01 s and 10.0 s (2008). *Earthquake Spectra*, 24(1), 99-138.
- [37] Dávalos H, Miranda E (2018). A ground motion prediction model for average spectral acceleration. *Journal of Earthquake Engineering*, 1-24.
- [38] Dávalos H, Heresi P, Miranda E (2020). A ground motion prediction model for *FIV3*. Submitted for publication to *Soil Dynamics and Earthquake Engineering*.
- [39] Almufti I, Motamed R, Grant DN, Willford M (2015). Incorporation of velocity pulses in design ground motions for response history analysis using a probabilistic framework. *Earthquake Spectra*, 31(3), 1647-1666.
- [40] Hayden CP, Bray JD, Abrahamson NA (2014). Selection of near-fault pulse motions. *Journal of Geotechnical and Geoenvironmental Engineering*, 140(7), 04014030.